

Article

Graft incompatibility between pepper and tomato elicits an immune response and triggers localized cell death

Hannah Rae Thomas ^{1,2,*}, Alice Gevorgyan^{1,3}, Alexandra Hermanson¹, Samantha Yanders¹, Lindsay Erndwein^{4,5}, Matthew Norman-Arztia¹, Erin E. Sparks⁴ and Margaret H. Frank^{1,*}

¹School of Integrative Plant Science, Cornell University, Ithaca, NY 14850, USA

²Department of Cell and Developmental Biology, John Innes Centre, Norwich NR2 2DT, UK

³Department of Biology, Stanford University, Stanford, CA 94305, USA

⁴Department of Plant and Soil Sciences, University of Delaware, Newark, DE 19713, USA

⁵Genetic Improvement for Fruits and Vegetables Laboratory, USDA-ARS, Chatsworth, NJ 08019, USA

*Corresponding authors. E-mail: Hannah.Thomas@jic.ac.uk; mh47@cornell.edu

Abstract

Graft compatibility is the capacity of two plants to form cohesive vascular connections. Tomato and pepper are incompatible graft partners; however, the underlying cause of graft rejection between these two species remains unknown. We diagnosed graft incompatibility between tomato and diverse pepper varieties based on weakened biophysical stability, decreased growth, and persistent cell death using viability stains. Transcriptomic analysis of the junction was performed using RNA sequencing, and molecular signatures for incompatible graft response were characterized based on meta-transcriptomic comparisons with other biotic processes. We show that tomato is broadly incompatible with diverse pepper cultivars. These incompatible graft partners activate prolonged transcriptional changes that are highly enriched for defense processes. Amongst these processes was broad nucleotide-binding and leucine-rich repeat receptors (NLR) upregulation and genetic signatures indicative of an immune response. Using transcriptomic datasets for a variety of biotic stress treatments, we identified a significant overlap in the genetic profile of incompatible grafting and plant parasitism. In addition, we found over 1000 genes that are uniquely upregulated in incompatible grafts. Based on NLR overactivity, DNA damage, and prolonged cell death, we hypothesize that tomato and pepper graft incompatibility is characterized by an immune response that triggers cell death which interferes with junction formation.

Introduction

Grafting is an ancient agricultural practice that is used to propagate plants and combine desirable traits between independent root and shoot systems [1–4]. The apical portion of a graft is known as the scion and the root system is known as the rootstock (Scion:Rootstock). Graft compatibility is defined by the ability of two individuals to form continuous vascular connections across the graft site [1, 5]. The inability to graft is categorized into two types of incompatibility: immediate incompatibility and delayed incompatibility [6, 7]. Delayed incompatibility can present months or years after grafting, with symptoms such as swollen, over-proliferated scions, cell death in the junction, and structural instability of the stem [8–10]. Graft compatibility is a significant issue for growers who rely on combining distinct species and varieties, through grafting, to alter plant architecture and increase disease resistance [11, 12]. Despite a long history of grafting, humans still struggle to understand the mechanisms underlying graft incompatibility. Currently, there are only a few examples where the causes of incompatibility have been identified [13–15]. Although there is likely a variety of species-specific cellular mechanisms that determine compatible versus incompatible graft pairings, the presence of persistent cell death in the junction is a common symptom that is observed across diverse plant families [9, 10].

Cell death can be classified into two main categories: necrosis and programmed cell death (PCD; [16]). Necrosis is defined as uncontrolled death and is often caused by stressors such as extreme heat, radiation, or a loss of membrane potential that is so intense that genetic processes are unable to act [16, 17]. In contrast, PCD is the controlled and organized process of cellular destruction [18].

All eukaryotes have evolved an innate immune system that is capable of detecting conserved foreign molecules during infection [19]. In plants, various elicitors such as pathogen associated molecular patterns (PAMPs) and damage-associated molecular patterns (DAMPs) are perceived by membrane bound pattern recognition receptors (PRRs) facing the apoplast [20–22]. These molecules trigger downstream pattern-triggered immunity (PTI) and signal basal defense processes such as reactive oxygen species (ROS) production [23]. Alternatively, some pathogens release effector proteins, which are expressed into the symplast to modify host responses and promote infection [24]. These effectors are locked in an arms race with intracellular nucleotide-binding and leucine-rich repeat receptors (NLRs), which perceive effectors or proteins modified by effectors and elicit effector-triggered immunity (ETI) and PCD [25]. Currently, no such molecules, apoplastic or symplastic, have been identified as the underlying

Received: 13 May 2024; Accepted: 2 September 2024; Published: 11 September 2024; Corrected and Typeset: 1 November 2024

© The Author(s) 2024. Published by Oxford University Press on behalf of Nanjing Agricultural University. This is an Open Access article distributed under the terms of the Creative Commons Attribution License (<https://creativecommons.org/licenses/by/4.0/>), which permits unrestricted reuse, distribution, and reproduction in any medium, provided the original work is properly cited.

cause of graft incompatibility, where an unknown signal from one graft partner is perceived by a protein of the other, thus leading to incompatibility.

Our previous work identified tomato and pepper as an herbaceous model for delayed incompatibility [26, 27]. Despite several studies investigating pepper graft compatibility, much remains unknown about the underlying mechanism [28–31]. To explore this, we grafted tomato to *Capsicum annuum* varieties, Cayenne, Doux des Landes, California Wonder, and *Capsicum chinense* variety Habanero. We found that tomato-*Capsicum* heterografts are all incompatible and exhibit failed xylem reconnections, weakened stem stability, and reduced growth. Using the tomato-pepper combination with the highest graft survival rate, tomato to California Wonder, we analyzed the presence of nonviable tissue (NVT) in the junction at 7, 14, and 21 days after grafting (DAG) and investigated the cause using viability staining and transcriptomics. In contrast to self-grafted controls which recover from cell death in the junction, we found that incompatible grafts exhibit persistent death. Additionally, we utilized RNA-sequencing to show that incompatible grafts have a prolonged defense response following grafting, including significant upregulation of many NLRs and important genetic components involved in defense response. Furthermore, we identified a set of potential incompatibility marker genes that are upregulated in incompatible junctions of both tomato and pepper stems. To characterize the molecular response of incompatible grafting in relation to other biotic stress responses, we conducted a transcriptomic meta-analysis comparing the effect of grafting with pathogen infection, herbivory, and plant parasitism. We found a significant overlap in expression patterns between grafting and plant parasitism, indicating similar mechanisms underpin interspecies plant-to-plant interactions. Lastly, we identified a suite of over 1000 genes that are uniquely upregulated in incompatible grafts but not other biological stressors; among these genes, we identified genetic processes involved in immune responses and DNA damage. Together, this work supports a model in which tomato and pepper grafts trigger an immune response including upregulated NLR expression, defensive compound production, and upregulation of genes associated with PCD, and DNA damage. This would be the first identified instance of an immunity based incompatibility in a cross-species grafted crop.

Results

Incompatible tomato and pepper heterografts are characterized by low survival, reduced growth, failed vascular connectivity, and physical instability

To investigate grafting between *Solanum lycopersicum* (tomato) and *Capsicum* (pepper) species, we performed a graft compatibility assay between self- and reciprocal grafts of *S. lycopersicum* var. M82 and *C. annuum* varieties Cayenne, Doux des Landes (DDL), California Wonder (CW), and *C. chinense* var. Habanero 30 days after grafting (DAG) (Figs S1 and S2; Table S1). Compared with self-grafted controls, heterografted tomato/pepper combinations exhibited significantly lower survival and higher break rates based on bend testing (Fig. S1a). Despite a low survival rate, self-grafted DDL plants that persisted formed strong graft junctions and were able to withstand the bend test [26, 27, 32]. Previous work reported DDL as a compatible graft partner with tomato, yet when we challenged the integrity of the graft using the bend test, the plants broke at the junction 92% of the time, indicating a high level of incompatibility that was previously undetected [28]. We

also analyzed growth of the grafted shoot and root systems to test for developmental restrictions. Compatible shoot and root systems were 92.7% and 38.2% larger than incompatible plants (Fig. S2a–b, Table S2). Additionally, the stem diameter of the scion was significantly restricted in their lateral development in incompatible grafts compared to self-grafted controls (Kruskal–Wallis Fig. S2c and d).

To examine the vascular connectivity of the grafts, we analyzed the anatomical organization of junctions from every tomato/pepper combination 30 DAG (Fig. 1). Consistent with our previous findings [26], all self-grafted combinations formed continuous xylem bridges across the graft junction (Fig. 1b, d, j, p, v, aa), demonstrating compatibility [27, 33, 34]. Tomato grafted to any of the pepper varieties formed nonvascular parenchymatous connections across the graft but failed to form xylem bridges (Fig. 1f, h, l, n, r, t, x, z, ab). We noticed that overproliferated scion callus (Fig. 1l, t, x), as well as adventitious root growth (Fig. 1f, n, t) were common features in these incompatible combinations.

Because CW exhibited high survival rates when heterografted with tomato, we selected this genotype for further analysis. Incompatible grafts are commonly discovered when the junction breaks, due to failed vascular connectivity or cell death in the junction [8–10]. With a better understanding of the vascular anatomy of compatible and incompatible plants, we sought to determine if we could quantify the instability observed in the manual bend test using a quantitative three-point bend test. Congruent with reduced biophysical stability observed with the three-point bend test, we found that there was a significant reduction in the structural stiffness of the heterografted junctions compared to self- and ungrafted stems (Fig. S3, Table S3).

Incompatible graft junctions accumulate significantly more NVT than compatible grafts

Cell death is a common symptom associated with incompatible grafts [32]. To examine the extent to which tomato/pepper (CW variety) heterografts exhibit elevated levels of cell death, we collected tissue from ungrafted tomato and pepper, self-graft tomato and pepper, and reciprocally heterografted tomato and pepper at 7, 14, and 21 DAG (Fig. S4). To quantify cell death in the junction, we used trypan blue staining to detect regions of cell death (Fig. 2, Table S4). We measured a 2.5 mm region of the hand sectioned junctions, including any callus present at the interface. When we considered just this sample area, the area of all graft junctions increased at a similar rate, independent of the stem diameter adjacent to the junction (Fig. S5a). When trypan blue stain is applied to thick tissue sections like this, regions where cell death are present in numerous tissue layers are visualized as blue-black under a light microscope. To quantify the percent of NVT versus viable tissue, we made a macro in ImageJ to extract tissue that was deeply stained with trypan blue (Fig. 2ak, Fig. S6) and divided this area by the entire area of the junction (Fig. S5b). We first analyzed ungrafted tomato (Fig. 2a, g, m) and pepper (Fig. 2b, h, n) stems that were the same age as the grafts we harvested at 7, 14, and 21 DAG. At most, the ungrafted stems from tomato and pepper contained 0.341% and 0.147% NVT respectively. Self-grafted tomato graft junctions consisted of 13.0% NVT at 7 DAG, which decreased to 3.51% by 21 DAG (Fig. 2u, aa, ag; Wilcoxon Paired Test $p=0.0589$). Similarly, self-grafted pepper junctions contained 24.8% NVT at 7 DAG but steadily decreased to only 2.92% by 21 DAG (Fig. 2v, ab, ah; $p=2.78E-02$). Unlike the self-grafts, which exhibited decreasing NVT over time, tomato:pepper and pepper:tomato incompatible grafts maintained a consistent percent of NVT over the 3-week sample period (Fig. 2s–aj). Tomato:pepper



Figure 1. Heterografted pepper fails to form vascular connections and shows a significant decrease in size 30 DAG. (a, c, e, g, i, k, m, o, q, s, u, w, y) Representative photographs and (b, d, f, h, j, l, n, p, r, t, v, x, z) confocal micrographs for self-grafted tomato (a, b), self-grafted habanero (c, d), tomato:Habanero (e, f), Habanero:tomato (g, h), self-grafted Doux des Landes (DDL) (i, j), tomato:DDL (k, l), DDL:tomato (m, n), self-grafted Cayenne (o, p), tomato:Cayenne (q, r), Cayenne:tomato (s, t), self-grafted California Wonder (CW) (u, v), tomato:CW (w, x), CW:tomato (y, z). Graft junctions were stained with propidium iodide and imaged on a confocal microscope. Pink arrows indicate a successful graft junction with a healed xylem (b, d, j, p, v, aa). White arrows indicate a failed vascular reconnection (f, h, l, n, r, t, x, z, ab) and white asterisk highlight adventitious roots (f, n, t). All plant image scale bars are 5 cm, and all micrograph scale bars are 1000 μm . (aa) A zoomed up view of self-grafted tomato to demonstrate successful xylem connections. (ab) A zoomed up view of heterograft tomato:cayenne junction to demonstrate failed xylem connections. Blue arrowheads denote xylem in the graft junction of aa and ab.

junctions contained 20.9%, 20.2%, and 20.8% NVT at 7, 14, and 21 DAG, respectively (Fig. 2w, ac, ai), and reciprocal pepper:tomato junctions exhibited similar levels of NVT: 21.9%, 17.9%, and 17.1%

NVT at 7, 14, and 21 DAG, respectively (Fig. 2x, ad, aj). Overall, tomato and pepper exhibited prolonged cell death up to 3 weeks post-grafting relative to self-grafted controls.

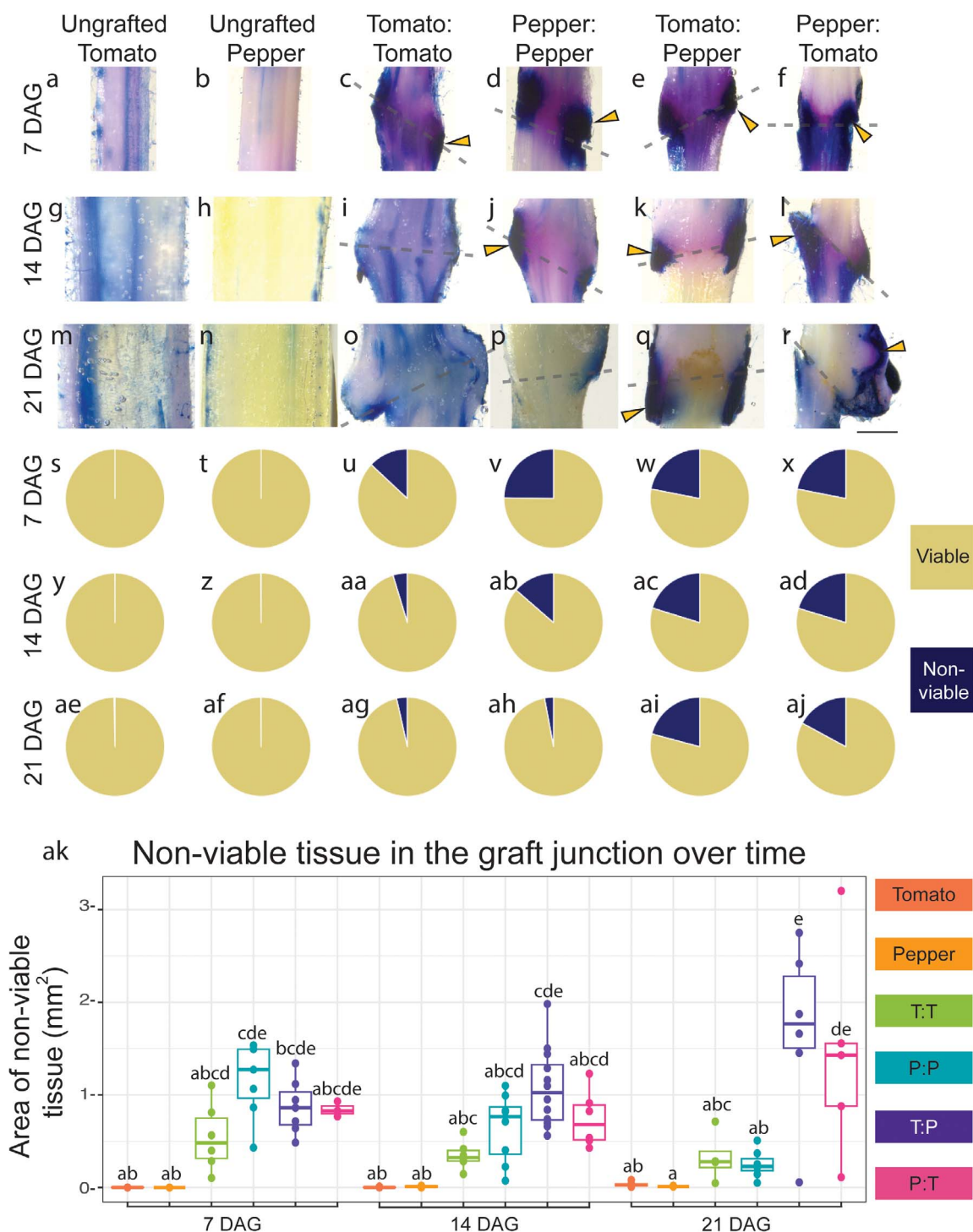


Figure 2. Incompatible grafts contain persistent NVT over time. (a–r) Representative images of 2.5 mm long graft junctions at 7, 14, and 21 DAG stained with Trypan Blue. A representative ungrafted tomato stem and the percent of NVT are shown at 7 DAG (a, s), 14 DAG (g, y), and 21 DAG (m, ae). A representative ungrafted pepper stem and the percent of NVT at 7 DAG (b, t), 14 DAG (h, z), and 21 DAG (n, af). A representative self-graft tomato junction and the percent of NVT at 7 DAG (d, v), 14 DAG (j, ab), and 21 DAG (o, ag). A representative self-grafted pepper junction and the percent of NVT at 7 DAG (e, w), 14 DAG (k, ac), and 21 DAG (q, ai). A representative pepper:tomato junction and the percent of NVT at 7 DAG (f, x), 14 DAG (l, ad), and 21 DAG (r, aj). Yellow arrows point to examples of tissue death; dashed lines signify the graft site; all junctions are 2.5 mm tall. All images set to same scale, with the scale bar equal to 1 cm (a–r). (s–aj) The percent of cell death and (ak) the area of cell death in the junction of all graft combinations at 7, 14, and 21 DAG. From left to right, dark orange depicts ungrafted tomato, light orange depicts ungrafted pepper, green depicts self-grafted tomato, teal depicts self-grafted pepper, purple depicts tomato:pepper, and pink depicts pepper:tomato. Compact letter display based on adjusted p-value of Tukey's HSD test. Biological replicates are depicted as jitter (ak) as well as described in detail in Table S4.

Previous work has attributed the incompatible symptom of NVT to the accumulation of trapped cellular debris that creates a necrotic layer in the graft [35]. However, the active accumulation of NVT through PCD provides an alternative explanation. To test whether NVT accumulation in incompatible grafts was due to PCD, we first attempted terminal deoxynucleotidyl transferase dUTP nick end labeling (TUNEL) assays, which labels double stranded DNA breaks, on graft junctions (Fig. S7-S9). Unfortunately, the high amount of developmental cell death due to vasculogenesis confounded our ability to quantify differences in PCD between compatible and incompatible grafts.

Next, to understand the cause of the NVT present in the incompatible grafts, we performed a preliminary assay to see if DAMPs, which activate DAMP-triggered immunity (DTI) upon cellular rupture during infection and herbivory, also play a role in determining incompatible species combinations [36–38]. To see if a component of one of the cell walls could act as an antagonist to inter-species grafting, we designed an *in vitro* assay to test for DAMP-induced changes in growth similar to work conducted in quince [14]. Tomato and pepper explants were allowed to grow on media containing either tomato or pepper wound exudates for 7 days. If wounding caused the secretion of an inhibitory chemical during callus formation, the hypocotyls growing on cross-species exudates would have altered growth. Despite a significant difference in overall growth rates between tomato and pepper explants, the presence of any cross-species DAMPs had no effect (Fig. S10, Table S5). Our results indicate that crude cross-species secreted exudates do not affect growth in this type of assay; however, this does not rule out the role of DAMPs in triggering graft incompatibility during other stages of junction formation.

Tomato and pepper heterografts express prolonged transcriptional defense profiles

To further investigate the underlying cause of NVT in incompatible grafts, we collected and performed RNA-sequencing on ungrafted, self-grafted, and heterografted tissue at 7, 14, and 21 DAG on tomato and CW pepper (Tables S6 and S7). When compared to ungrafted stems, self-grafted junctions expressed 4.5x, 5x, and 15x less differentially expressed genes compared to heterografts at 7, 14, and 21 DAG, respectively (Fig. 3, Tables S8 and S9). The reduced number of differentially expressed genes in self-grafts correlates with the healing timeline, where compatible tomato and pepper self-grafts heal within the first week [27].

To identify genes uniquely up- and down-regulated in the incompatible grafts, we used likelihood ratio testing (Table S10 and S11). Distinct genes were upregulated in the scion and stock, with only a fraction in common at any time point, suggesting that the genetic response in incompatible grafts is spatially and temporally regulated (Fig. S11a-f). For example, at 7 DAG, 1530 and 2380 genes were uniquely upregulated in the scion and stock of incompatible tomato grafts (Fig. S11). Of these 3910 genes, only 576 were shared between scion and stock. The percent of genes upregulated in the scion that were also upregulated in stock for tomato was only 38%, 2%, and 11% of the total scion DEGs at 7, 14, and 21 DAG, respectively. Similarly, genes upregulated in the pepper scion that were also upregulated in the stock made up only 6%, 29%, and 17% of the total scion genes at 7, 14, and 21 DAG. Additionally, scion tissue shared more genes across time than stocks, further supporting that the position in relation to the graft junction, holds a significant role in the genetic process (Fig. S11g-j).

Using significantly upregulated genes from either tomato:pepper or pepper:tomato incompatible graft combinations, we performed

GO term enrichment (Fig. 4a,b, S12–S13, Tables S12 and S13). Downregulated genes showed few conserved trends across time points and species (Fig. S13), but we found that processes associated with defense and stress displayed the highest enrichment in upregulated genes from heterografted tomato stocks 14 DAG and pepper stocks 7 DAG (Fig. 4a, b). To further explore how defense processes might be involved in the incompatible response, we targeted NLRs and downstream molecular signaling involved in defense for deeper analysis. Using a collection of 320 previously annotated tomato NLRs [39], we identified 97 defense-related receptors that were significantly upregulated in incompatible grafts (Fig. 4c, Table S14). Of these 97 NLRs, 82 were upregulated in the pepper:tomato 14 DAG sample, indicating this is a critical time point for activating defense-related molecular responses during incompatibility. Similarly, 145 of the 356 annotated pepper NLRs were upregulated during incompatible grafting (Fig. 4d), with a pronounced molecular signature of 101 NLRs upregulated in tomato:pepper grafts 7 DAG [40]. Notably, stock tissue from both tomato and pepper incompatible grafts exhibit highly upregulated NLR expression within the first 2 weeks post-grafting (Fig. 4a-b). In the absence of an effector protein or pathogen, overexpression of NLRs can trigger autoimmunity that leads to hypersensitive response (HR; [41]). To test whether cell death in incompatible grafts could result from HR or other defense processes, we analyzed the expression of tomato and pepper orthologs EDS1, SAG101, and PAD4, which are known regulators in Arabidopsis (Fig. 4e, Table S14; [42–44]). Again, we identified incompatible graft-specific upregulation, especially at 14 DAG, for these regulators (Fig. 4e).

Next, to explore the role of hormonal regulation in graft compatibility, we identified the closest tomato and pepper putative homologs for annotated Arabidopsis genes involved in salicylic acid (SA), jasmonic acid (JA), and ethylene biosynthesis and response (Fig. S14a–c, Table S14). All three of these hormones are known to play a role in defense processes, with SA serving a critical function in NLR-induced HR and immunity [45–47]. In addition, JA and ethylene are associated with graft junction formation [27, 48]. At 7 DAG, SA, JA, and ethylene biosynthesis were upregulated in all grafted samples relative to ungrafted controls, indicating that hormonal signaling is prominent early in healing. By 14 and 21 DAG, SA, JA, and ethylene biosynthesis and perception were predominantly upregulated in the incompatible scions compared to self-grafted controls (Fig. S14). Congruent with this response, we noticed that the tomato and pepper orthologs for PR1, a defense gene downstream of SA signaling, was upregulated at 21 DAG in incompatible scions (Fig. S14a). The expression of these genes three-weeks after grafting indicates that the prolonged incompatible graft response is related to defense processes which may be activated or mediated by SA, JA, and ethylene hormonal pathways.

Another hormonal-regulated defense process that was significantly enriched across our incompatible graft time points was the biosynthesis of steroidal glycoalkaloids (SGAs; Fig. 5a, Table S14). SGAs are a class of jasmonate-dependent defensive compounds produced by Solanaceous species [49–52]. Upon further investigation, we were able to find that many genes in SGA biosynthesis (GAME1,4,6,7,11,12,17,18, and MKB1) were significantly upregulated in the incompatible tissue, especially in the scion [53]. Since this response is shared in tomato and pepper, it is possible that SGA biosynthesis could be triggered by the graft incompatibility immune response [54]. Furthermore, SGA content could be a useful metric for gauging graft compatibility in Solanaceae.

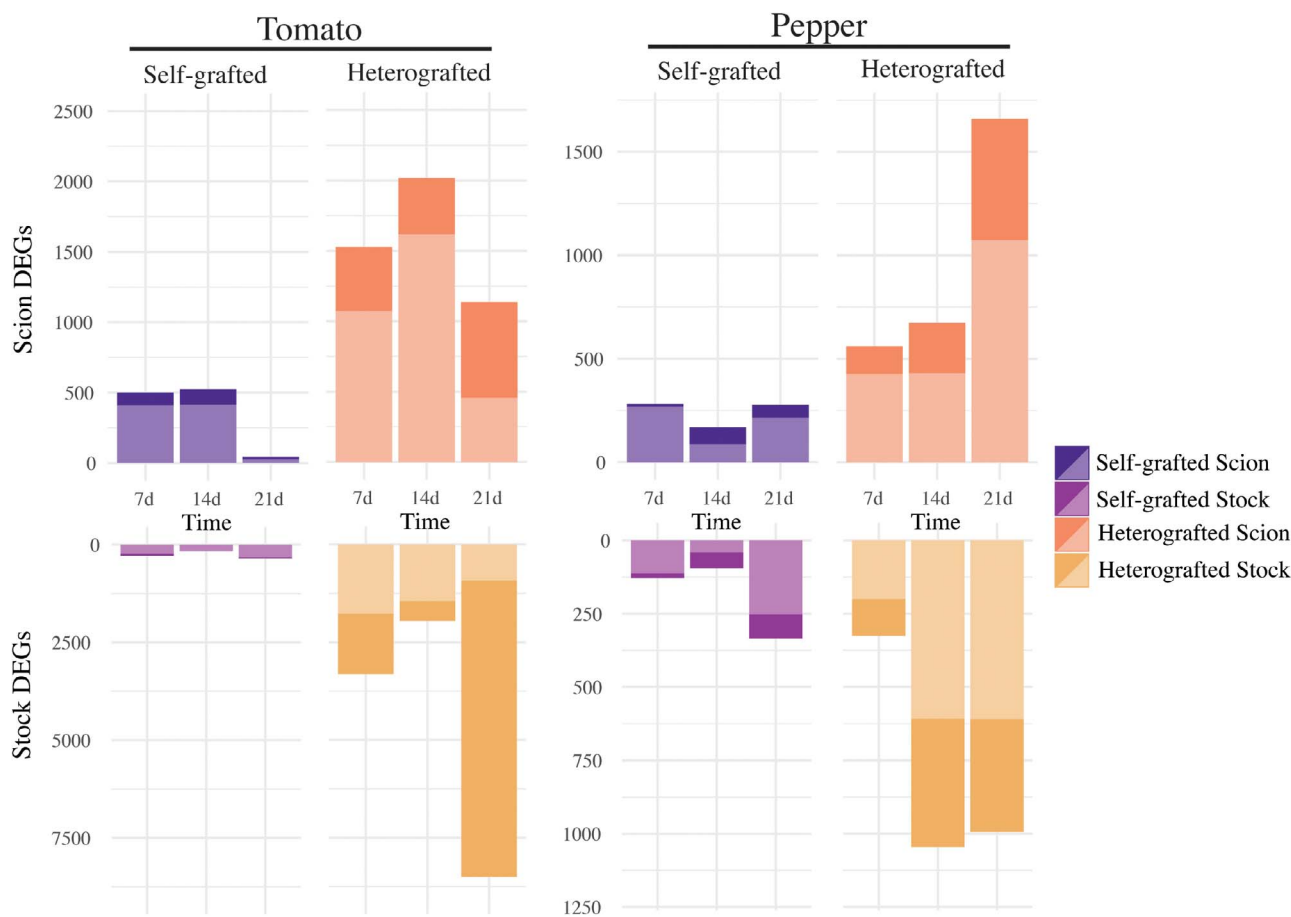


Figure 3. Incompatible heterografts have prolonged differential gene regulation compared to self-grafts. Differentially expressed genes ($|1.5|$, adjusted p -value < 0.05) of each grafted tissue (compared to ungrafted) at each time point for tomato and pepper. Upregulated genes are shown in light colors and downregulated genes are shown in dark colors. Self-grafted scions are dark purple, self-grafted stocks are light purple, heterografted scions are orange, and heterograft stocks are yellow. Each combination has 3–5 bio-replicates.

We also explored molecular markers for ROS production. We examined the expression profiles of known RBOHs [55, 56] and found that of the 8 RBOHs annotated in tomato, only SIRBOH1 and SIRBOHF were both upregulated in incompatible tissue (Fig. S14d, Table S14). Surprisingly, none of the antioxidant enzymes previously shown to be upregulated alongside RBOHs were significantly upregulated in any of our incompatible grafts [56]. This data suggested that ROS production is not a dominant by-product of tomato–pepper graft incompatibility at 7 DAG and beyond.

Additionally, we observed that the stocks of incompatible grafts exhibited high levels of RNA degradation, as determined by low alignment rates, especially at 21 DAG (Table S15). RNA degradation over time in incompatible tissue might be a by-product of genotoxic stress or DNA damage as a part of PCD [57, 58]. We also found that orthologs of genes shown to act as markers of developmental PCD (i.e., SCPL48, BFN1, DMP2) and biotic stress induced PCD (i.e., HSF1, WRKY75, ISTL6) in Arabidopsis were upregulated in at least one time point of heterografted tomato (Table S10; [59]). Although our TUNEL assays were inconclusive due to the confounding effects of vasculogenesis during graft formation, this data provides molecular support for the role of PCD in both promoting persistent cell death in incompatible tomato–pepper grafts through a biotic stress induced mechanism, in addition to protoxylem development.

Another interesting group of genes uniquely upregulated in the incompatible grafts were identified plant homologs to BREAST

CANCER SUSCEPTIBILITY GENE 1 (BRCA1, Solyc09g066080, Solyc12g041980) and BRCA1 ASSOCIATED RING DOMAIN PROTEIN 1 (BARD1, Solyc05g016230; Table S22). In mammals, these genes form a homodimer that is required for homologous recombination, a mode of DNA repair following genotoxic stress. Homologous recombination is a less common method of DNA repair in eukaryotes, whereas nonhomologous end joining is the most prevalent mode. Regardless, the Arabidopsis paralogs for BRCA1/BARD1 are upregulated by genotoxic damage, so it is possible that a graft-induced immune response in incompatible grafts leads to DNA damage which triggers BRCA1/BARD1.

To determine whether incompatible graft response genes were conserved between tomato and pepper genomes, we generated strict orthogroups between tomato, pepper, and Arabidopsis (Table S16) and used previously published orthogroupings [27]. We then identified significantly upregulated genes (between grafted versus ungrafted controls) with shared ortholog groupings in both tomato and pepper (Table S17–S18). For instance, out of the 1074 and 428 genes upregulated in the heterografted scions of tomato:pepper and pepper:tomato at 7 DAG, there were 69 orthogroups conserved between the two species. We identified relatively more shared orthogroups in incompatible graft samples versus self-grafted controls, especially with respect to incompatible scion samples (Fig. 5b). Even when considering the magnitude of DEGs between samples, the number of shared orthogroups

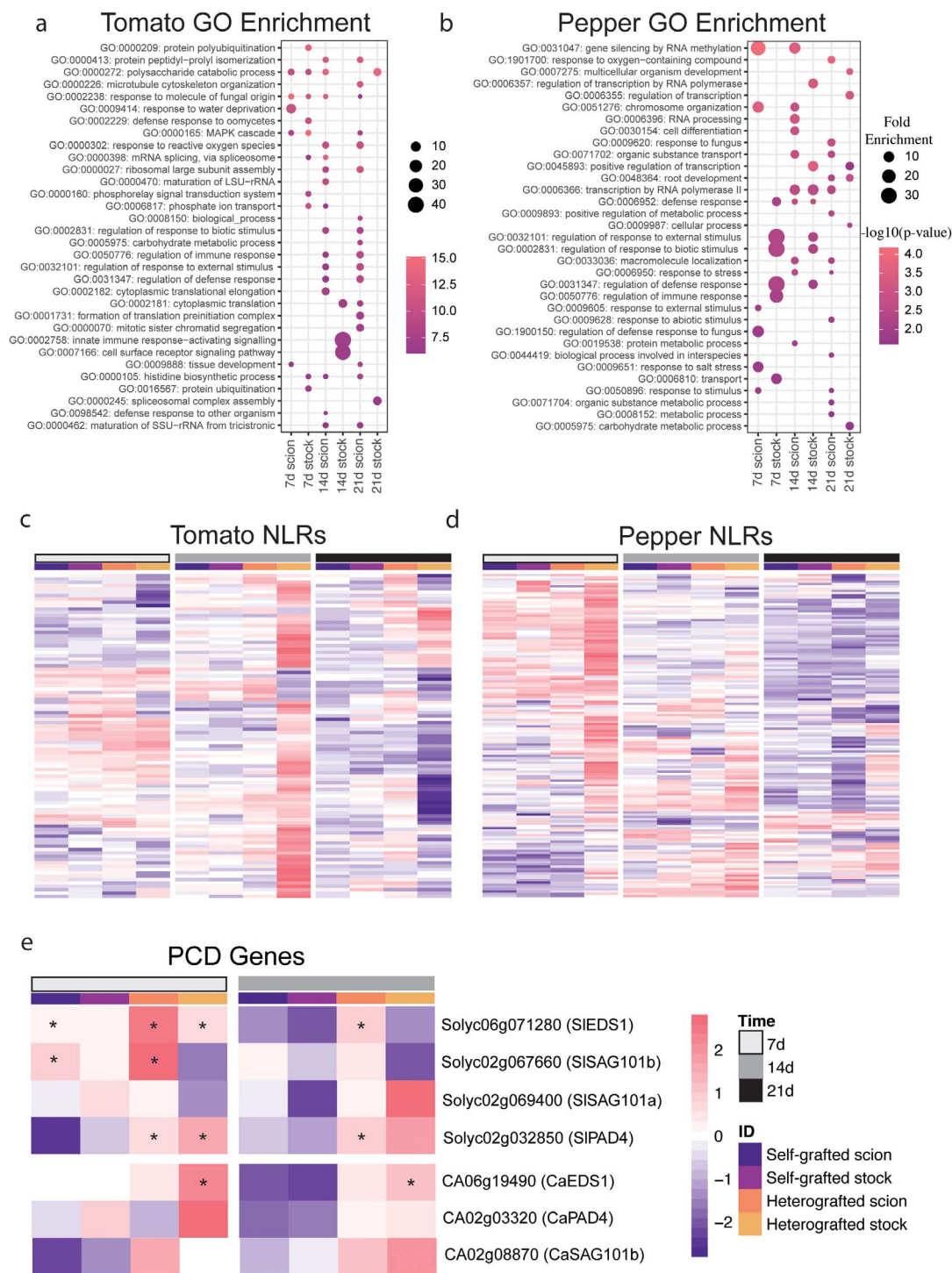


Figure 4. Incompatible graft-specific upregulated genes are involved in defense response. (a, b) Uniquely upregulated incompatible graft genes were determined by performing likelihood ratio testing ($p < 0.05$) on ungrafted, self-graft scion, and incompatible graft scion as well as ungrafted, self-grafted stock, and incompatible stock tissue. The genes upregulated in only the incompatible graft tissue were used to perform GO enrichment. GO terms enriched in incompatible grafted tomato tissue at 7, 14, and 21 DAG (a). GO terms enriched in incompatible grafted pepper tissue at 7, 14, and 21 DAG (b). (c, d) Log-fold change of NLRs in grafted tissue compared to ungrafted tissue of tomato (c) and pepper (d). (e) The log-fold change of genes involved in hypersensitive response in grafted vs. ungrafted tissue. The log-fold change was scaled by row. The tissue is denoted by the colored columns, from left to right, where self-grafted scions are dark purple, self-grafted stocks are light purple, incompatible grafted scions are orange, and incompatible grafted stocks are yellow. The days after grafting were denoted by colored columns, from left to right, where 7 DAG are white, 14 DAG are grey, and 21 DAG are black. Asterix denotes adjusted P -value < 0.05 and log-fold change greater than $|1.5|$.

in incompatible tissue remains proportionately higher than self-grafted tissue. Previous work has shown that tomato and pepper reads incorrectly cross-map to each other's genomes less

than $< 10\%$ of the time, supporting this data [27]. This finding indicates that molecular responses to incompatibility share a high degree of overlap between the tomato and pepper genomes. From

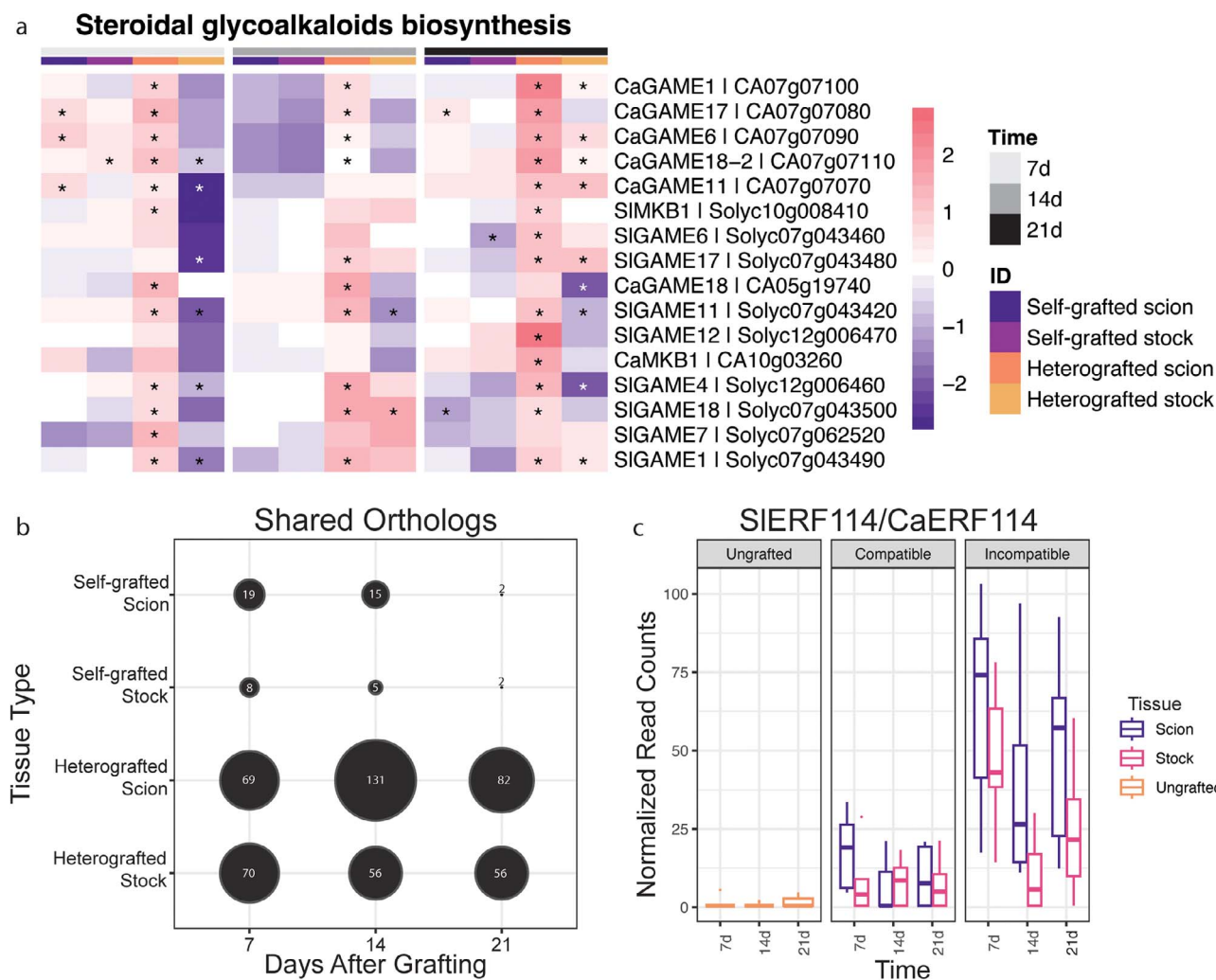


Figure 5. The steroidal glycoalkaloid biosynthesis pathway among significantly upregulated processes in heterografted grafted scions. (a) Upregulated genes for all graft combinations were determined in comparison to ungrafted stems, from left to right, at 7 (light grey), 14 (dark grey), and 21 (black) DAG in the self-grafted scion (dark purple), self-grafted stock (magenta), heterografted scion (orange), and heterografted stock (yellow). Significant differential expression qualified by LFC greater than $|1.5|$ and adjusted p -value <0.05 . Significance is denoted with an asterisk. (b) Orthologs upregulated at any given tissue/time point in both tomato and pepper. Orthogroups were determined between *Solanum lycopersicum*, *Capsicum annuum*, and *Arabidopsis thaliana* using OrthoFinder. Upregulated genes for all graft combinations were determined in comparison to ungrafted stems. Each gene had a corresponding orthogroup. A shared ortholog was determined if upregulated genes (lfc >1.5 , adjusted <0.05) from both tomato and pepper at a common tissue/time point were linked to the same orthogroup. (c) Normalized read counts of SIERF114 and CaERF114 were across time. Read counts for tomato and pepper were normalized and faceted by tissue type. Box plots of ungrafted tissue read counts are orange, boxplots of scions tissue read counts are purple, and boxplots of stock tissue read counts are pink.

this analysis, we identified ERF114 (Soly03g118190/CA03g31320) as a shared orthogroup that is upregulated in incompatible grafts at 7, 14, and 21 DAG. ERF114 is closely related to RAP2.6 L (RELATED to AP2.6 L; Fig. 5c), a wound-responsive transcription factor that exhibits overlapping expression with auxin depletion and high levels of JA in stock tissue within the first 24 hours of grafting [60–62]. Similar to RAP2.6 L, AtERF114 has been shown to be upregulated under high JA and involved in graft junctions formation [61, 63]. Incompatible-specific upregulation of Sl/CaERF114 could be explained by the role of AtERF114 in ectopic xylem and lateral root formation in *Arabidopsis* [64]. This hypothesis is supported by the formation of unorganized overproliferated xylem tissue in the incompatible grafts, many of which produce adventitious roots (Fig. 1). These orthologs, much like SGA biosynthesis, serve as candidate markers for detecting incompatibility in Solanaceae.

Incompatible grafting upregulates a set of unique defense processes

Our analyses of incompatible graft responses indicate that both tomato and pepper upregulate strong disease resistance-related molecular responses. To test whether this response is specific to incompatible grafting, or whether these genes share overlapping functions with plant immunity and defense, we compared upregulated incompatible grafting genes with published datasets of three biotic stressors: early plant parasitism [65], insect herbivory [66], and established necrotrophic fungal infections (47 hours post-inoculation; [67]). We also used an arbuscular mycorrhizal symbiosis dataset as a control for nondestructive biotic processes [68]. Despite these processes occurring in differing tissues and developmental stages, all datasets were moderately correlated with all 7 DAG tomato samples (Spearman Rank average correlation; 0.58; Fig. 6a) and we were able to identify shared

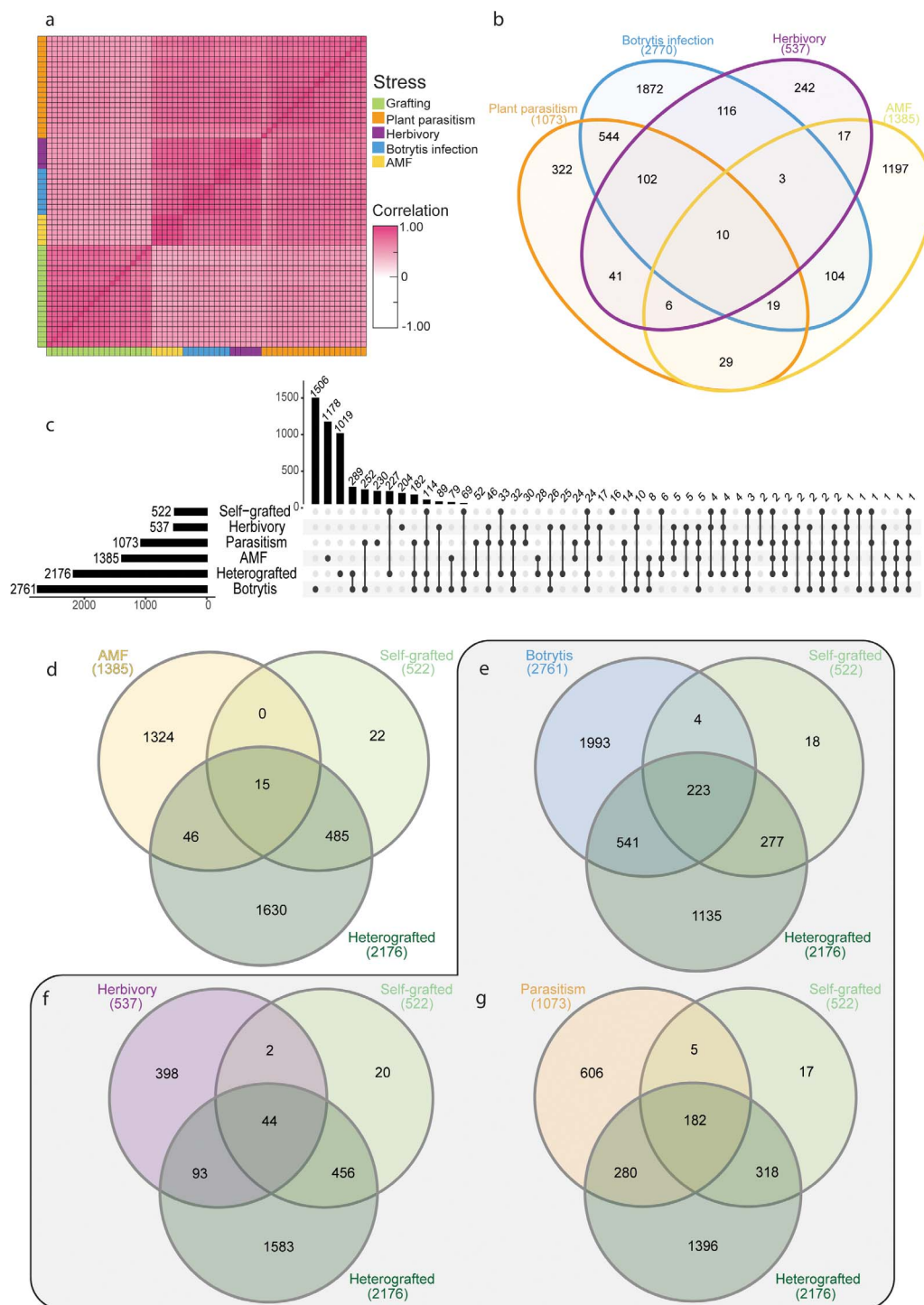


Figure 6. Grafting elicits unique and shared genetic processes with other biological stressors. (a) Spearman Rank Correlation between 7 DAG samples, botrytis infection, herbivory, plant parasitism, and arbuscular mycorrhizal fungi (AMF) colonization. (b) Overlap of upregulated genes from four biological processes investigated. (c) Upset plot showing the overlap between upregulated genes from the biological processes: AMF, plant parasitism, insect herbivory, and fungal infection, scion or stock self-, and scion or stock incompatible-grafted tissue at 7 DAG and all biological processes. (d–g) Overlap of upregulated genes from scion or stock of self- or incompatible-grafted tissue at 7 DAG and all biological processes. (d) The overlap between grafting and AMF, (e) botrytis fungal infection, (f) herbivory, (g) and plant parasitism. The grey outline denotes the biological stressors, whereas AMF was used as a control.

transcriptional responses with grafted plants (Fig. 6d–g), as well as between different biotic treatments (Fig. 6b, Table S19). Additionally, all stressors were found to have a significant representation factor (RF) greater than 1 with self- and heterografted tissue; meaning that there was a significantly increased overlap of genes upregulated in the stressed tissue

and the grafted tissue than expected by chance (Fisher's Exact Test with hypergeometric probability; Table S20). This is in comparison to the arbuscular mycorrhizal fungi (AMF) dataset, which contained 1385 significantly upregulated genes but lacked enriched overlap with self- or heterografted tissue (Fig. 6d).

Amongst the three biotic stressors analyzed, the necrotrophic fungi, *Botrytis cinerea*, elicited the highest transcriptional responses with 2761 differentially upregulated genes. 223 of these genes were also upregulated in self and incompatible grafts. 541 genes were upregulated in only infected and incompatible grafted tissue (RF: 2.2, Fig. 6e). Shared genes were involved in defense-related processes such as RLKs, MAP kinases, LRR proteins, and cell death, such as HSR4 (Solyc02g062550; Table S21; [69]). Plants stressed with herbivory by the tobacco hornworm (*Manduca sexta*) expressed 537 upregulated genes (Fig. 6f). Of these, 44 were shared between herbivory, self-and incompatible grafted plants, 2 were uniquely shared with self-grafted datasets (RF:5.9), and 93 were uniquely shared with incompatible grafts (RF:1.9).

The parasitic plant, *Cuscuta campestris*, led to 1073 upregulated DEGs, of which 182 are shared between parasitized, self-, and incompatible grafted tissue (Fig. 6g). 280 genes were both upregulated in only parasitized tissue and incompatible grafts (RF:3.2), while 5 were upregulated in both parasitized and self-grafted but not incompatible grafts (RF:6.4). The developmental and anatomical processes of parasitic haustorium formation and graft formation share strong parallels; both structures involve tissue reunion and the patterning of newly formed vascular connections. Given these parallels, we hypothesized that parasitism would have the greatest overlap in DEGs with grafted stems, which we found to be especially true for compatible grafts (total gene overlap, RF:5.7). Surprisingly, parasitism also shared the most significant overlap with incompatible grafts out of all three biotic stress treatments (total gene overlap, RF: 3.4). Enriched processes in parasitized, self- and heterografted plants include polysaccharide catabolic processes, response to molecules of fungal origin, defense response to other organisms, and cellular response to oxygen-containing compounds. Genes from these categories include Pathogenesis-related (PR) genes, endochitinases, chitinases, and ethylene biosynthesis components. Genes upregulated in both parasitized tissue and incompatible grafts were enriched for GO terms such as MAPK cascades, regulation of defense responses, regulation of immune response, and defense response to other organisms suggesting that both incompatible grafting and plant parasitism elicit interspecies defense responses.

While we identified a significant overlap between self-, incompatible grafts, and tissue subjected to the three biotic stressors, we also identified a large set of genes that were uniquely upregulated in grafted samples only (Figs 6c, S16). Self- and incompatible grafts uniquely upregulated 227 genes, and incompatible grafts alone expressed a unique signature of 1019 upregulated genes. These genes were enriched for GO terms including polysaccharide catabolic process and anthocyanin biosynthesis, ABA/salt stress/drought, salicylic acid perception, and response to oxidative stress (Table S22). Within these genes, we identified the putative tomato ortholog to AtWRKY70 (Solyc03g095770), which functions at the interface of SA and JA signaling [70], in incompatible graft samples at 7 and 14 DAG. Interestingly, the grape ortholog to AtWRKY70 (VIT_08s0058g01390) was previously identified as an upregulated gene in incompatible grape grafts [71], making this gene an extremely interesting candidate for future studies in graft incompatibility. In summary, we found that grafting, especially incompatible grafts share significant genetic overlap with other biotic stressors which trigger well-studied immune responses. We also found that incompatible grafts elicit unique transcriptional programming distinct from other processes such as infection or herbivory, suggesting that novel processes are stimulated during graft incompatibility.

Discussion

In this study, we use an expanded set of germplasm (four pepper varieties from two different *Capsicum* species) to demonstrate that tomato and pepper are broadly incompatible. This assessment is based on the formation of weak graft junctions and failed vascular reconnections between all tomato/pepper combinations (Figs 1, S1–S3). Notably, previous literature cited the Doux des Landes (DDL) pepper variety as graft-compatible with tomato [28]. This historic assessment was likely based on high survival rates between tomato:DDL combinations. Recent work has emphasized the role of secreted β -1,4-glucanases in initial graft adhesion of Solanaceous species [72]. It is possible that the DDL pepper variety has altered extracellular secretions that reduce self-graft rates. Regardless, we demonstrated that along with all other varieties of pepper tested, tomato-DDL grafts fail to form xylem bridges, and as a consequence, develop biophysically unstable junctions that fail the bend test. Based on our findings, we emphasize the importance of verifying anatomical connectivity when diagnosing graft compatibility, and we recommend additional analyses investigating xylem formation and long-term productivity, to unambiguously assess compatible combinations. For all of the heterografts tested, we also were able to show that vascular bridges were not formed and growth was reduced (Figs 1, S1–S3).

In order to analyze cell death in the graft junction, we tracked the percent of NVT during the first 3 weeks postgrafting (Fig. 2). All grafts exhibited elevated NVT at 7 DAG, compatible grafts exhibited reduced NVT at 14 and 21 DAG, while incompatible grafts maintained the same percentage of NVT over time. Historically, cell death in the graft junction has been referred to as necrotic tissue [73]. We believe that this term fails to capture the true nature of the cellular death within an incompatible graft. Unlike necrosis, which is uncontrolled acute cell death, PCD is an important genetic mechanism that allows for selective cell destruction. In addition to its function in developmental processes (e.g., tracheid and vessel element maturation), PCD plays a central role in defense, including HR. To investigate the cause of sustained NVT in incompatible grafts and to determine if PCD was involved, we used RNA-seq to analyze the molecular signature of compatible versus incompatible grafts (Fig. 3). In addition to the incompatible grafts displaying a prolonged transcriptional response up to 21 DAG compared to self-grafts, genes upregulated at these time points were enriched for processes associated with defense. Of these upregulated incompatible genes were many NLRs (Fig. 4). NLRs form complexes that monitor both effector presence and effector mediated changes to other proteins; when activated, NLRs trigger ETI and downstream defense responses [74]. NLRs can also self-activate, triggering an inappropriate immune response [75, 76]. This phenomenon was originally identified as a type of genetic incompatibility present in F1 offspring of interspecific crosses, leading to the name “hybrid necrosis” [77]. Plants executing this immune response display cell death lesions, reduced growth, yellowing, and even complete death [78]. This phenomenon is now attributed to an autoactivated immune response. The neofunctionalization of NLRs in individual species has led to expanded and diverse families, which when crossed can interact deleteriously, activating defense responses in a similar mode to pathogen triggered defense [76]. The expression of NLRs must remain tightly controlled, since upregulation leads to serious growth penalties [79]. Furthermore, overexpression of NLRs can be sufficient to activate autoimmunity [80]. Like instances of plant autoimmunity, we found significant upregulation of the NLRs from both tomato and pepper in

incompatible grafts [81]. It is possible that components of the immune systems are scion-to-stock graft-mobile, thus triggering an immune response which broadly upregulates NLRs in the incompatible grafted stocks leading to a type of autoimmunity induced cell death. This would be the first instance of autoimmunity triggered by physical rather than reproductive genomic combinations. Given that the graft junction is composed of an interspecific fusion of tissues, where the genetic information of tomato and pepper are in intimate proximity, it is logical that grafting could elicit an immune response. Indeed, this idea has been posited before by Dontcho Kostoff in 1928, where he questioned the ability of interspecies grafts to generate antibodies [73, 82]. While we now know that plants do not pose the immunogenic capacity to generate antibodies, this work supports a hypothesis of complex non-self detection in interspecies grafted plants.

We found that the cell death present in the junction shared genetic similarities to HR. HR requires salicylic acid and a core set of genes *PAD4*, *SAG101*, and *EDS1* in *Arabidopsis*. We found that most of the orthologs to these regulators, in addition to SA responsive genes, were upregulated in incompatible grafts compared to self-grafted controls (Fig. 4, S14a). Future work investigating the role these genes play in tomato-pepper graft incompatibility will further elucidate this graft-immunity phenomenon. Our molecular evidence points to a model in which tomato-pepper graft incompatibility is caused by an immune response activated by incompatible immune systems, which triggers cell death in the junction. This immune response and subsequent cell death within the junction likely interferes with the proper signaling and nutritional coordination required by the scion and stock to heal the graft. An alternative hypothesis is that the immune response follows a failed physiological reconnection of grafted tissues. Further work looking at the early temporal healing will help resolve these processes.

We also identified a set of shared orthologs that are upregulated in both the tomato and pepper genomes during incompatible grafting. Further analysis of these shared orthologs may help to identify genetic markers for incompatibility in Solanaceae and beyond (Fig. 5).

Lastly, to explore the genetic fingerprint of graft incompatibility, we compared upregulated genes from compatible grafts, incompatible grafts, and three biotic stress datasets (herbivory, fungal infection, and plant parasitism; Fig. 6). We identified an overlap between grafting and these biotic stressors, with a significantly pronounced overlap of upregulated genes between grafting and plant parasitism. Given that the formation of the parasitic haustorium and the graft junction both require inter-specific tissue coordination leading to vascular reconnection, it is logical that the two processes share molecular machinery [83]. The similarity between these two phenomena, both genetically and physiologically, will require future research to fully explore. This analysis revealed over 1000 uniquely upregulated genes that are expressed in incompatible grafts, including DNA damage repair genes, *BRCA1* and *BARD1* (Fig. 6c).

Conclusion

Previous work has shown NLR overactivation can induce DNA damage via *EDS1* [58]. In a similar process, we propose that tomato and pepper grafting elicits an immune response, which upregulates hundreds of NLRs, and induces the accumulation of NVT in incompatible graft junctions. Further supporting our model, these incompatible grafts shared a unique upregulation

of DNA damage repair and HR-related genes that are associated with immune responses. From this analysis, we have identified a cross-species induced immune response as the likely cause for tomato-pepper graft incompatibility and cell death.

Materials and methods

Plant materials and growth conditions

C. annuum var. California Wonder (CW), RC Cayenne (Cayenne), Doux des Landes (DDL), and *C. chinense* var. Habanero and *C. chinense* (pepper), and *S. lycopersicum* (tomato) seeds were used for graft compatibility screening (Method S1). 21-day-old pepper seedlings and 14-day-old tomato seedlings were grafted (Method S2 and S3).

Characterizing graft compatibility

30 DAG, the vascular connectivity of tomato and pepper junctions were assayed using propidium iodide staining (Method S4). Graft junction integrity was tested using manual bending [27]. (Method S5). *C. annuum* var. CW and *S. lycopersicum* Var. M82 were used to conduct three-point bend tests at the University of Delaware. Structural mechanics of the graft junction were assessed by three-point bend testing (Method S6) [84–86].

DAMP assay

Hypocotyl explants from *C. annuum* var. CW and *S. lycopersicum* Var. M82 were placed on callus-inducing media for 7 days (Method S7). The hypocotyl tissue was then placed onto media which either previously cultured tomato or pepper tissue for 7 additional days. The area of the explants was measured after 7 days on the experimental media.

Grafting for TUNEL, trypan blue staining, and RNA-seq

C. annuum var. (CW) and *S. lycopersicum* Var. M82 were grown as described above. Thirty-six of each tomato and pepper species were left ungrafted. The rest of the plants were grafted as described above in the following combinations: 50 tomato:tomato, 50 CW:CW, 70 tomato:CW, and 70 CW:tomato. Ungrafted CW and tomato plants were included in the recovery procedure. Plastic domes were vented 7 DAG and removed 14 DAG.

Trypan blue staining

Stems from 7, 14, 21 DAG, and ungrafted plants were collected and stained with 1% Trypan Blue, as previously reported (Method S8; [87]).

TUNEL assay

A 0.5-cm piece of the junction from 7, 14, 21 DAG, and ungrafted plants were used to image PCD. Assays were performed using the Promega DeadEnd™ Fluorometric TUNEL System (Method S9).

Transcriptomic analysis

C. annuum var. CW and *S. lycopersicum* Var. M82 were grafted, as previously described. A 0.5 cm of the junctions of 7, 14, 21 DAG, and ungrafted plants were collected from five biological replicates for each sample. Each piece of tissue was flash-frozen and ground with a mortar and pestle. Total RNA was purified and 3' Seq libraries were constructed at the Cornell Institute of Biotechnology, Biotechnology Resource Center, and the libraries were sequenced on an Illumina NextSeq 500/550 using an Illumina High-output kit (Method S10). Fasta files were processed to yield raw reads and differential expression

analysis was performed using DESeq2 (Method S10; [88]). Putative orthogroups were determined using OrthoFinder with Diamond as the sequence search program (Method S11; [89, 90]). Publicly available RNA-seq data were downloaded and processed to yield raw read counts (Method S12).

Statistical analysis and image analysis

All statistical computation and graph generation were performed in R v4.1.2 [91] (Method S13).

Acknowledgements

H.R.T. was supported by a United States Department of Agriculture National Institute of Food and Agriculture (USDA-NIFA) Predoctoral Fellowship (2020-67011-31882); M.H.F., A.G., S.P., and M.N. were supported by the National Science Foundation (NSF) (CAREER IOS-1942437) and by a U.S.-Israel Binational Science Foundation grant (2019192). Imaging data was acquired through the Cornell Institute of Biotechnology's Imaging Facility, with NIH (S10OD018516) funding for the shared Zeiss LSM880 confocal/multiphoton microscope. Access to the Instron Universal testing stand was supported by the Delaware Center for Musculoskeletal Research from the National Institute of Health's National Institute of General Medical Sciences (P20GM139760). Thank you to Noor AlBader for assistance with data transfer.

Author contributions

H.R.T. and M.H.F. designed the study. H.R.T., A.G., A.H., S.Y., L.E., M.N., and E.S. carried out the experimentation. H.R.T. analyzed the data. H.R.T. wrote the first draft of the manuscript. All authors contributed critically to the final draft and approval publication.

Data availability

RNA reads collected for this project have been deposited on NCBI GEO (GSE256079). Previously published RNA-seq data used in this research can be accessed on NCBI at PRJNA628162, PRJNA687611, PRJNA756681, PRJNA600385, and PRJNA773605.

Conflict of interest statement

None to declare.

Supplementary Data

Supplementary data is available at *Horticulture Research* online.

References

- Harrison DJ, Burgess PG. Use of rootstock resistance for controlling fusarium wilt of tomatoes. *Plant Pathol.* 1962;**11**:23–5
- Mudge K, Janick J, Scofield S. et al. A History of Grafting. In: *Hortic Rev.* 2009;437–93
- Warschefsky EJ, Klein LL, Frank MH. et al. Rootstocks: diversity, domestication, and impacts on shoot phenotypes. *Trends Plant Sci.* 2016;**21**:418–37
- Williams B, Ahsan MU, Frank MH. Getting to the root of grafting-induced traits. *Curr Opin Plant Biol.* 2021;**59**:101988
- Moore R. A model for graft compatibility-incompatibility in higher plants. *Am J Bot.* 1984;**71**:752–8
- Argles GK. A review of the literature on stock-scion incompatibility in fruit trees: with particular reference to pome and stone fruits. Imperial Bureau of Fruit Production. 1937.
- Mendel K. The anatomy and histology of the bud-union in citrus. *Palest J Bot Hortic Sci.* 1936;**1**:13–46
- Andrews PK, Marquez CS. Graft incompatibility. In: *Hortic Rev.* 2010;183–232
- Eames AJ, Cox LG. A remarkable tree-fall and an unusual type of graft-union failure. *Am J Bot.* 1945;**32**:331–5
- Moore R, Walker DB. Studies of vegetative compatibility-incompatibility in higher plants. II. A structural study of an incompatible heterograft between *sedum telephoides* (crassulaceae) and *Solanum pennellii* (solanaceae). *Am J Bot.* 1981;**68**:831–42
- Webster AD Vigour mechanisms in dwarfing rootstocks for temperate fruit trees. *Acta Horticulturae* 658. 2004
- King SR, Davis AR, Liu W. et al. Grafting for disease resistance. *HortScience.* 2008;**43**:1673–6
- Gur A. The role of the cyanogenic glycoside of the quince in the incompatibility between pear cultivars and quince rootstocks. *Hortic Res.* 1968;**8**:113–34
- Moore R. Graft incompatibility between pear and quince: the influence of metabolites of *Cydonia oblonga* on suspension cultures of *Pyrus communis*. *Am J Bot.* 1986;**73**:1–4
- Mosse B, Herrero J. Studies on incompatibility between some pear and quince grafts. *J Hortic Sci.* 1951;**26**:238–45
- Burbridge E, Diamond M, Dix PJ. et al. Use of cell morphology to evaluate the effect of a peroxidase gene on cell death induction thresholds in tobacco. *Plant Sci.* 2007;**172**:853–60
- Hirsch T, Marchetti P, Susin SA. et al. The apoptosis-necrosis paradox. Apoptogenic proteases activated after mitochondrial permeability transition determine the mode of cell death. *Oncogene.* 1997;**15**:1573–81
- Lockshin RA, Zakeri Z. Apoptosis, autophagy, and more. *Int J Biochem Cell Biol.* 2004;**36**:2405–19
- Janeway C, Travers P, Walport M. et al. *Immunobiology: The Immune System in Health and Disease* Vol. 2. New York: Garland Pub; 2001:154
- Amarante-Mendes GP, Adjemian S, Branco LM. et al. Pattern recognition receptors and the host cell death molecular machinery. *Front Immunol.* 2018;**9**:2379
- Jones JDG, Dangl JL. The plant immune system. *Nature.* 2006;**444**:323–9
- Steinbrenner AD, Muñoz-Amatriáin M, Chaparro AF. et al. A receptor-like protein mediates plant immune responses to herbivore-associated molecular patterns. *Proc Natl Acad Sci USA.* 2020;**117**:31510–8
- Boller T, He SY. Innate immunity in plants: an arms race between pattern recognition receptors in plants and effectors in microbial pathogens. *Science.* 2009;**324**:742–4
- Stergiopoulos I, de Wit PJGM. Fungal effector proteins. *Annu Rev Phytopathol.* 2009;**47**:233–63
- Wu L, Chen H, Curtis C. et al. Go in for the kill: how plants deploy effector-triggered immunity to combat pathogens. *Virulence.* 2014;**5**:710–21
- Thomas HR, Gevorgyan A, Frank MH. Anatomical and biophysical basis for graft incompatibility within the Solanaceae. *J Exp Bot.* 2023;**74**:4461–70
- Thomas H, Van den Broeck L, Spurney R. et al. Gene regulatory networks for compatible versus incompatible grafts identify a role for SlWOX4 during junction formation. *Plant Cell.* 2022;**34**:535–56

28. Deloire A, Héban C. Peroxidase activity and lignification at the Interface between stock and Scion of compatible and incompatible grafts of capsicum on *Lycopersicum*. *Ann Bot*. 1982;**49**: 887–91
29. Ives L, Brathwaite R, Barclay G. et al. Graft compatibility of scotch bonnet (*Capsicum chinense* Jacq) with selected salt-tolerant solanaceous. *J Agric Sci Technol B*. 2012;**2**:81–92
30. Kawaguchi M, Taji A, Backhouse D. et al. Anatomy and physiology of graft incompatibility in solanaceous plants. *J Hort Sci Biotechnol*. 2008;**83**:581–8
31. Zeist AR, Giacobbo CL, da Silva Neto GF. et al. Compatibility of tomato cultivar Santa Cruz Kada grafted on different Solanaceae species and control of bacterial wilt. *Hortic Bras*. 2018;**36**:377–81
32. Moore R. Studies of vegetative compatibility-incompatibility in higher plants. Iv. The development of tensile strength in a compatible and an incompatible graft. *Am J Bot*. 1983;**70**:226–31
33. Melnyk CW, Schuster C, Leyser O. et al. A developmental framework for graft formation and vascular reconnection in *Arabidopsis thaliana*. *Curr Biol*. 2015;**25**:1306–18
34. Moore R. Graft compatibility and incompatibility in higher plants. *Dev Comp Immunol*. 1981;**5**:377–89
35. Tiedemann R. Graft union development and symplastic phloem contact in the heterograft *Cucumis sativus* on *Cucurbita ficifolia*. *J Plant Physiol*. 1989;**134**:427–40
36. Brutus A, Sicilia F, Macone A. et al. A domain swap approach reveals a role of the plant wall-associated kinase 1 (WAK1) as a receptor of oligogalacturonides. *Proc Natl Acad Sci USA*. 2010;**107**: 9452–7
37. Ferrari S, Savatin DV, Sicilia F. et al. Oligogalacturonides: plant damage-associated molecular patterns and regulators of growth and development. *Front Plant Sci*. 2013;**4**:49
38. Nothnagel EA, McNeil M, Albersheim P. et al. Host–pathogen interactions. XXII. A galacturonic acid oligosaccharide from plant cell walls elicits phytoalexins. *Plant Physiol*. 1983;**71**:916–26
39. Bashir S, Rehman N, Fakhar Zaman F. et al. Genome-wide characterization of the gene family in tomato and their relatedness to disease resistance. *Front Genet*. 2022;**13**:931580
40. Lee H, Mang H, Choi E. et al. Genome-wide functional analysis of hot pepper immune receptors reveals an autonomous NLR clade in seed plants. *New Phytol*. 2021;**229**:532–47
41. Freh M, Gao J, Petersen M. et al. Plant autoimmunity-fresh insights into an old phenomenon. *Plant Physiol*. 2022;**188**:1419–34
42. Gantner J, Ordon J, Kretschmer C. et al. An EDS1-SAG101 complex is essential for TNL-mediated immunity. *Plant Cell*. 2019;**31**: 2456–74
43. Rietz S, Stamm A, Malonek S. et al. Different roles of enhanced disease Susceptibility1 (EDS1) bound to and dissociated from phytoalexin Deficient4 (PAD4) in *Arabidopsis* immunity. *New Phytol*. 2011;**191**:107–19
44. Zhu S, Jeong R-D, Venugopal SC. et al. SAG101 forms a ternary complex with EDS1 and PAD4 and is required for resistance signaling against turnip crinkle virus. *PLoS Pathog*. 2011;**7**:e1002318
45. Enyedi AJ, Yalpani N, Silverman P. et al. Localization, conjugation, and function of salicylic acid in tobacco during the hypersensitive reaction to tobacco mosaic virus. *Proc Natl Acad Sci USA*. 1992;**89**:2480–4
46. Koornneef A, Pieterse CMJ. Cross talk in defense signaling. *Plant Physiol*. 2008;**146**:839–44
47. Lorenzo O, Piqueras R, Sánchez-Serrano JJ. et al. Ethylene response factor1 integrates signals from ethylene and jasmonate pathways in plant defense. *Plant Cell*. 2003;**15**:165–78
48. Wang J, Li D, Chen N. et al. Plant grafting relieves asymmetry of jasmonic acid response induced by wounding between scion and rootstock in tomato hypocotyl. *PLoS One*. 2020;**15**:e0241317
49. Cárdenas PD, Sonawane PD, Pollier J. et al. GAME9 regulates the biosynthesis of steroidal alkaloids and upstream isoprenoids in the plant mevalonate pathway. *Nat Commun*. 2016;**7**:10654
50. Itkin M, Heinig U, Tzfadia O. et al. Biosynthesis of antinutritional alkaloids in solanaceous crops is mediated by clustered genes. *Science*. 2013;**341**:175–9
51. Milner SE, Brunton NP, Jones PW. et al. Bioactivities of glycoalkaloids and their aglycones from *Solanum* species. *J Agric Food Chem*. 2011;**59**:3454–84
52. Panda S, Jozwiak A, Sonawane PD. et al. Steroidal alkaloids defence metabolism and plant growth are modulated by the joint action of gibberellin and jasmonate signalling. *New Phytol*. 2022;**233**:1220–37
53. Nakayasu M, Shioya N, Shikata M. et al. JRE4 is a master transcriptional regulator of defense-related steroidal glycoalkaloids in tomato. *Plant J*. 2018;**94**:975–90
54. Abdelkareem A, Thagun C, Nakayasu M. et al. Jasmonate-induced biosynthesis of steroidal glycoalkaloids depends on COI1 proteins in tomato. *Biochem Biophys Res Commun*. 2017;**489**: 206–10
55. Li X, Li Y, Ahammed GJ. et al. RBOH1-dependent apoplastic H₂O₂ mediates epigallocatechin-3-gallate-induced abiotic stress tolerance in *Solanum lycopersicum* L. *Environ Exp Bot*. 2019;**161**:357–66
56. Raziq A, Wang Y, Mohi Ud Din A. et al. A comprehensive evaluation of salt tolerance in tomato (Var. Ailsa Craig): responses of physiological and transcriptional changes in RBOH's and ABA biosynthesis and signalling genes. *Int J Mol Sci*. 2022;**23**:1603
57. Nisa M-U, Huang Y, Benhamed M. et al. The plant DNA damage response: signaling pathways leading to growth inhibition and putative role in response to stress conditions. *Front Plant Sci*. 2019;**10**:653
58. Rodriguez E, Chevalier J, El Ghouli H. et al. DNA damage as a consequence of NLR activation. *PLoS Genet*. 2018;**14**:e1007235
59. Olvera-Carrillo Y, Van Bel M, Van Hautegeem T. et al. A conserved core of programmed cell death indicator genes discriminates developmentally and environmentally induced programmed cell death in plants. *Plant Physiol*. 2015;**169**:2684–99
60. Asahina M, Azuma K, Pitaksaringkarn W. et al. Spatially selective hormonal control of RAP2.6L and ANAC071 transcription factors involved in tissue reunion in *Arabidopsis*. *Proc Natl Acad Sci USA*. 2011;**108**:16128–32
61. Lakehal A, Dob A, Rahnesan Z. et al. Ethylene response factor 115 integrates jasmonate and cytokinin signaling machineries to repress adventitious rooting in *Arabidopsis*. *New Phytol*. 2020;**228**:1611–26
62. Matsuoka K, Yanagi R, Yumoto E. et al. RAP2.6L and jasmonic acid-responsive genes are expressed upon *Arabidopsis* hypocotyl grafting but are not needed for cell proliferation related to healing. *Plant Mol Biol*. 2018;**96**:531–42
63. Zhang A, Matsuoka K, Kareem A. et al. Cell-wall damage activates DOF transcription factors to promote wound healing and tissue regeneration in *Arabidopsis thaliana*. *Curr Biol*. 2022;**32**:1883–1894.e7
64. Canher B, Lanssens F, Zhang A. et al. The regeneration factors ERF114 and ERF115 regulate auxin-mediated lateral root development in response to mechanical cues. *Mol Plant*. 2022;**15**: 1543–57
65. Jhu M-Y, Farhi M, Wang L. et al. Investigating host and parasitic plant interaction by tissue-specific gene analyses on tomato and

- Interface at three Haustorial developmental stages. *Front Plant Sci.* 2021;**12**:764843
66. Ke L, Wang Y, Schäfer M. et al. Transcriptomic profiling reveals shared signalling networks between flower development and herbivory-induced responses in tomato. *Front Plant Sci.* 2021;**12**: 722–810
67. Srivastava DA, Arya GC, Pandaranayaka EP. et al. Transcriptome profiling data of *Botrytis cinerea* infection on whole plant *Solanum lycopersicum*. *Mol Plant-Microb Interact.* 2020;**33**:1103–7
68. Zeng Z, Liu Y, Feng X-Y. et al. The RNAome landscape of tomato during arbuscular mycorrhizal symbiosis reveals an evolving RNA layer symbiotic regulatory network. *Plant Commun.* 2023;**4**:100429
69. Zhang B, Van Aken O, Thatcher L. et al. The mitochondrial outer membrane AAA ATP ase at OM 66 affects cell death and pathogen resistance in *Arabidopsis thaliana*. *The Plant Journal.* 2014;**80**:709–27
70. Li J, Brader G, Kariola T. et al. WRKY70 modulates the selection of signaling pathways in plant defense. *Plant J.* 2006;**46**:477–91
71. Assunção M, Santos C, Brazão J. et al. Understanding the molecular mechanisms underlying graft success in grapevine. *BMC Plant Biol.* 2019;**19**:396
72. Notaguchi M, Kurotani KI, Sato Y. et al. Cell-cell adhesion in plant grafting is facilitated by β -1, 4-glucanases. *Science.* 2020;**369**: 698–702
73. Kostoff D. Studies on callus tissue. *Am J Bot.* 1928;**15**:565–76
74. Jones JDG, Vance RE, Dangl JL. Intracellular innate immune surveillance devices in plants and animals. *Science.* 2016;**354**: 1117–25
75. Bomblies K, Lempe J, Epple P. et al. Autoimmune response as a mechanism for a Dobzhansky-Muller-type incompatibility syndrome in plants. *PLoS Biol.* 2007;**5**:e236
76. Tran DTN, Chung E-H, Habring-Müller A. et al. Activation of a plant NLR complex through Heteromeric association with an autoimmune risk variant of another NLR. *Curr Biol.* 2017;**27**: 1148–60
77. Hollingshead L. A lethal factor in *Crepis* effective only in an interspecific hybrid. *Genetics.* 1929;**15**:114–40
78. Bomblies K, Weigel D. Hybrid necrosis: autoimmunity as a potential gene-flow barrier in plant species. *Nat Rev Genet.* 2007;**8**:382–93
79. Tian D, Traw MB, Chen JQ. et al. Fitness costs of R-gene-mediated resistance in *Arabidopsis thaliana*. *Nature.* 2003;**423**:74–7
80. Lai Y, Eulgem T. Transcript-level expression control of plant NLR genes. *Mol Plant Pathol.* 2018;**19**:1267–81
81. Barragan AC, Collenberg M, Wang J. et al. A truncated singleton NLR causes hybrid necrosis in *Arabidopsis thaliana*. *Mol Biol Evol.* 2021;**38**:557–74
82. Kostoff D. Acquired immunity in plants. *Genetics.* 1929;**14**:37–77
83. Kurotani KI, Wakatake T, Ichihashi Y. et al. Host-parasite tissue adhesion by a secreted type of β -1, 4-glucanase in the parasitic plant *Phtheirospermum japonicum*. *Commun Biol.* 2020;**3**:407
84. Ennos AR, Crook MJ, Grimshaw C. The anchorage mechanics of maize, *Zea mays*. *J Exp Bot.* 1993;**44**:147–53
85. Goodman AM, Ennos AR. The effects of mechanical stimulation on the morphology and mechanics of maize roots grown in an aerated nutrient solution. *Int J Plant Sci.* 2001;**162**:691–6
86. Hostetler AN, Erndwein L, Ganji E. et al. Maize brace root mechanics vary by whorl, genotype, and reproductive stage. *Ann Bot.* 2022;**126**:657–68
87. Fernández-Bautista N, Domínguez-Núñez JA, Moreno MMC. et al. Plant tissue trypan blue staining during phytopathogen infection. *Bio-protocol.* 2016;**6**:e2078–8
88. Love MI, Huber W, Anders S. Moderated estimation of fold change and dispersion for RNA-seq data with DESeq2. *Genome Biol.* 2014;**15**:550
89. Buchfink B, Xie C, Huson DH. Fast and sensitive protein alignment using diamond. *Nat Methods.* 2014;**12**:59–60
90. Emms DM, Kelly S. OrthoFinder: phylogenetic orthology inference for comparative genomics. *Genome Biol.* 2019;**20**:238
91. R Core Team. R: A Language and Environment for Statistical Computing. R Foundation for Statistical Computing; 2021: